sciendo

DOI: 10.2478/ata-2025-0022

Acta Technologica Agriculturae 3
Nitra, Slovaca Universitas Agriculturae Nitriae, 2025, pp. 176–182

IMPROVING THE ACCURACY OF AIR TEMPERATURE MONITORING FOR AUTOMATED TASKS IN AGRICULTURE USING AFFORDABLE METEOROLOGICAL EQUIPMENT

Zuzana Ságová[1], Pavel Kuznetsov[2, 3], Vladyslav Evstigneev[2], Tibor Krenický*[4], Dmitriy Voronin[2, 3], Dmitriy Kotelnikov[2, 3], Boris Yakimovich[2]

[1]University of Žilina, Faculty of Mechanical Engineering, Department of Automation and Production Systems, Žilina, Slovakia, zuzana.sagova@fstroj.uniza.sk
[2]Sevastopol State University, Institute of Nuclear Energy and Industry, Department of Electric Power Engineering, Sevastopol, Crimea, pavelnik2@gmail.com (P.K.), vald_e@rambler.ru (V.E.), yakimovich52@gmail.com (B.Y.)
[3]National Research Centre "Kurchatov Institute" – "Magarach", Laboratory of Digital Technologies in Winemaking and Viticulture, Yalta, Crimea, voronin@sevsu.ru (D.V.), dykotelnikov@ya.ru (D.K.)
[4]Technical University of Košice, Faculty of Manufacturing Technologies, Department of Technical Systems Design and Monitoring, Prešov, Slovakia
*correspondence: tibor.krenicky@tuke.sk

This study examines methods for improving air temperature measurement accuracy in agriculture using affordable meteorological equipment. Experimental results demonstrate that non-aspirated radiation shields introduce systematic measurement errors of up to 3 °C during daylight hours due to solar radiation heating. Two error mitigation approaches were evaluated: an aspirated shield system and a mathematical correction algorithm based on solar radiation intensity and wind speed measurements. The developed correction model, incorporating radiation shield geometry and heat transfer dynamics, reduced measurement deviations to 0.5–0.6 °C. The comparative analysis of data collected at Sevastopol meteorological station (June–August 2023) revealed a superior performance of the mathematical correction method (RMSE 0.17 °C, KGE 0.993) compared to the aspirated shield solution. The proposed correction algorithm achieves measurement accuracy within World Meteorological Organisation (WMO) standards without additional mechanical components that compromise system reliability. These findings facilitate the development of cost-effective distributed meteorological monitoring networks applicable to precision agriculture operations.

Keywords: radiation shield bias; temperature sensors; meteorological instrumentation; heat transfer modelling; precision agriculture; thermal correction algorithms

Data on weather conditions take an important place in the list of critical information needed for decision making in agriculture (Frisvold and Murugesan, 2013). Producers are more likely to use meteorological data for timing of planting, cultivation, prevent diseases, and harvest across diverse areas of agricultural production (Onesti et al., 2016; Chen et al., 2021; Kuznetsov et al., 2022; Marmai et al., 2022; Zhang et al., 2023). The recent studies reveal a problem of climate change impact on farm future planning which highlights the necessity of local dense and high-performance meteorological sensors networks to anticipate potential threats (Holleman et al., 2020). Automated weather stations are effective tools for monitoring meteorological parameters enabling to implement a concept of "precision agriculture" (Ammoniaci et al., 2021; El Hachimi et al., 2023). The main advantages of such systems are related to the capability of local monitoring across the farm field, increased sampling of meteorological data, low cost, and relative ease of deploying a sensor network using IoT technology (Ferrández-Pastor et al., 2018; Ioannou et al., 2021).

Air temperature is one of the key parameters. Its accurate measurement is complicated by solar radiation influence, which causes additional heating of radiation shields, leading to systematic measurement errors (da Cunha, 2015; Sun et al., 2015). The analysis of temperature measurement accuracy when using various radiation shields revealed that some of them can introduce significant bias of up to several degrees when exposed to solar radiation (Erell et al., 2005; Hubbard and Lin, 2002; Tarara and Hoheisel, 2007).

The main methods for enhancing the precision of air temperature measurement under intense solar radiation are: using aspirated radiation shields or calibrating measurements based on data regarding solar radiation intensity and other relevant factors (Georges and Kaser, 2002; Richardson et al., 1999; Yang et al., 2016). The utilisation of aspirated shields significantly reduces the bias associated with additional heating (Jenkins, 2014; Yang et al., 2012), while calibration using the mathematical models of heat balance allows for the correction of sensor readings (Dai et al., 2023; Yang et al., 2018; Yang et al., 2021; Hubbart, 2011).

While previous studies have demonstrated the integration of various systems, they have not fully explored the potential of high-performance systems as proposed in this study. Therefore, we investigated

the effectiveness of existing methods for improving the accuracy of air temperature measurements using affordable meteorological devices.

Material and methods

Monitoring meteorological characteristics in agriculture requires low-cost automated information-measuring systems with spatially distributed sensors (Matese et al., 2009; Ali et al., 2024). These systems integrate reference meteorological devices with cost-effective sensors to obtain detailed meteorological data at micro and meso scales. To evaluate temperature measurement bias in affordable meteorological devices, an experimental stand was constructed comprising two meteorological complexes with different radiation shields: non-aspirated (NASP) and aspirated (ASP). The stand was installed at Sevastopol meteorological station on Pavlovsky Cape. The block diagram of the experimental bench is illustrated in Fig. 1.

The study was conducted in two phases. In the first phase, the efficacy of the ASP shield was assessed and potential bias in ambient temperature readings was measured by comparing both meteorological devices against reference data (RD). The second phase involved the evaluation of the NASP radiation shield with an adaptive algorithm (NASPa) for adjusting measurements based on solar radiation intensity and wind speed measurements from a "Sokol-M1" module equipped with an anemometer and pyranometer.

Standard meteorological equipment installed according to WMO guidelines at Sevastopol meteorological station provided RD for surface air temperature (Fig. 2). This equipment featured a precision temperature recorder with ±0.1 °C accuracy, operating at 2 m height as specified by WMO (2023). The intercomparison was conducted from 1 June to 31 August 2023. The bias for each meteorological device under study was assessed based on the RD.

Both ASP and NASP experimental devices utilised SHTC3 temperature sensors with ±0.2 °C accuracy, operating range from -40 to 125 °C, and 3.3–5.5 V power requirements. These sensors recorded values every 15–20 seconds, and the data was transferred to a server for visualisation and storage. Measurements were then converted to hourly averages (±1 minute around each hour) to facilitate comparison between RD and sensor measurements.

Both ASP and NASP weather devices employed ABS plastic radiation shields (140 mm outer diameter, 62 mm inner diameter, 85 mm height) with stacked horizontal plates for airflow optimisation while blocking direct radiation. The radiation shield comprised 6 horizontal plates made of light ivory ABS plastic with a slightly conical shape, spaced approximately 12 mm apart. This configuration optimises natural ventilation while effectively preventing direct solar radiation from reaching the temperature sensor. The ASP configuration integrated a 50 mm electric fan (1 W) powered by a 5 W polycrystalline PV module via an MPPT controller (CN3767). This design ensures operational autonomy through a self-regulating mechanism where fan speed varies proportionally with solar radiation intensity, enabling the system to adapt automatically to changing environmental conditions.

For storage and processing of measured data, the meteorological complexes are equipped with a transmitting device capable of continuous data transmission to a web server via the Internet. This enables remote access to meteorological measurements and facilitates data visualisation. Figure 3 illustrates the functional diagram of a meteorological device assembled with inexpensive components.

The Sokol-M measurement module features comprehensive wind monitoring capabilities. For airflow velocity, the instrument operates within a 1–60 $m \cdot s^{-1}$ measurement range with 0.1 $m \cdot s^{-1}$ resolution. Measurement accuracy varies by velocity range: ±0.5 $m \cdot s^{-1}$ within 1–5 $m \cdot s^{-1}$, and ±(0.5 + 0.05 V) $m \cdot s^{-1}$ at higher velocities (where

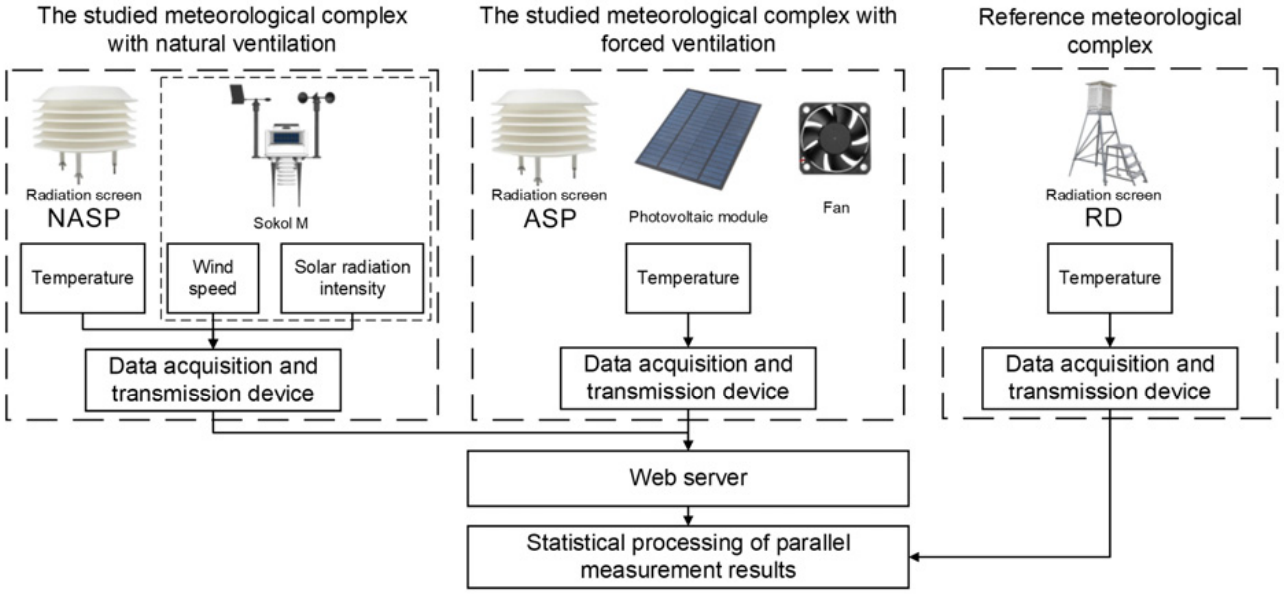


Fig. 1 Structural diagram of the experimental bench



Fig. 2 Photo from the meteorological station
(a) general view; (b) detail

V represents the measured value). The directional measurement system provides full 360-degree coverage with ±3 degrees absolute accuracy and 1-degree resolution. Directional measurements initiate at a minimum threshold of 0.8 $m \cdot s^{-1}$ airflow velocity, ensuring reliable orientation data.

Mathematical post-processing was implemented to account for influencing factors, including radiation shield type, solar radiation intensity, and wind speed (Hubbard et al., 2001). A filtering algorithm was employed to exclude statistical outliers using a confidence interval approach where measurements exceeding 3x standard deviation from the mean were removed. For each meteorological parameter, a minimum of 50 discrete measurements were collected before applying the filtering procedure, ensuring a robust statistical reliability of the processed data and minimising sampling error effects.

Theoretical framework for measurement adjustment

The accuracy enhancement of air temperature measurements using NASP shields can be achieved by compensating systematic errors associated with radiation shield heating. This correction utilises simultaneous measurements of wind flow velocity and solar radiation intensity.

A new universal air temperature correction formula is proposed based on the fundamental heat balance equation (1):

$$Q_{in} - Q_{out} = 0 \qquad (1)$$

where: Q_{in} – amount of heat entering the radiation shield (J); Q_{out} – amount of heat removed from the radiation shield (J)

Heat entering the radiation shield is determined by solar radiation intensity, surface albedo, and exposed area (2):

$$Q_{in} = (1 - A) \cdot IS \cdot F_1 \cdot \tau \qquad (2)$$

where: A – surface albedo; IS – solar radiation intensity ($W \cdot m^{-2}$); F_1 – surface area exposed to solar radiation (m^2); τ – time (s)

To simplify the mathematical model, focus was placed on convective heat exchange and thermal conductivity as the dominant heat removal mechanisms. Radiative heat transfer and other less influential mechanisms were not directly modelled; instead, their combined effect was approximated using an empirical nonlinearity coefficient (ε) within a modified Newton-Richmann equation (3):

$$Q_{out} = (\Delta T \cdot h \cdot F_2 + \varepsilon \cdot F_3) \cdot \tau \qquad (3)$$

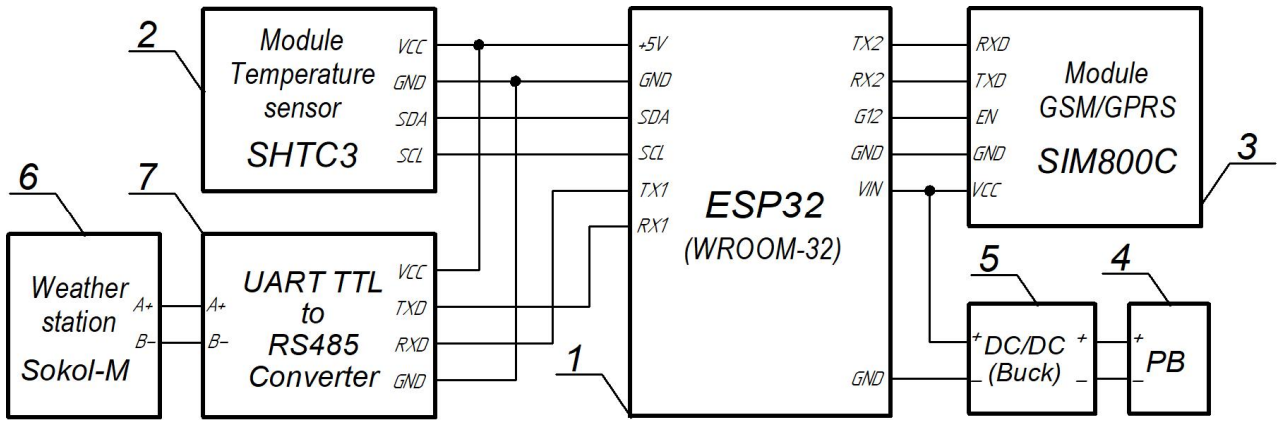


Fig. 3 Meteorological complex components
1 – ESP32 microcontroller; 2 – SHTC3 temperature sensor; 3 – SIM800C GSM/GPRS module; 4 – Li-ion battery; 5 – DC/DC converter; 6 – "Sokol-M" measuring module; 7 – UART-RS485 interface

where: ΔT – sensor temperature deviation (K); h – heat transfer coefficient from the radiation shield to the environment (W·m^{-2}·K^{-1}); F_2 – wind-blown surface area (m^2); ε – empirical nonlinearity coefficient of heat transfer (W·m^{-2}); F_3 – total surface area (m^2)

Combining Eqs (1)–(3) one can yield the formula for temperature deviation ΔT:

$$\Delta T = \frac{(1-A)\cdot IS\cdot F_1 - \varepsilon\cdot F_3}{h\cdot F_3} \quad (4)$$

The total heat transfer coefficient combines forced (h_w) and free (h_f) convection components:

$$h = h_w + h_f \quad (5)$$

where: h_w – forced convection heat transfer coefficient (W·m^{-2}·K^{-1}); h_f – free convection heat transfer coefficient (W·m^{-2}·K^{-1})

The empirical nonlinearity coefficient can be introduced as follows:

$$\varepsilon = k\left(\frac{IS}{IS_{STC}}\right)^{1.2} \quad (6)$$

where: k – stands for empirical thermal correction coefficient (W·m^{-2}); IS_{STC} – intensity of solar radiation under standard conditions (1000 W·m^{-2}) (Hubbard and Lin, 2002)

Heat transfer coefficients for forced (h_w) and free (h_f) convection were determined using standard dimensionless numbers Nusselt, Reynolds, Prandtl, and Grashof according to classical heat transfer theory (Bergman and Lavine, 2017). The forced convection coefficient utilises the relationship between Reynolds number (depended on wind speed) and the Prandtl number of air, while free convection incorporates Grashof number effects related to buoyancy forces.

After substituting these relationships and relevant parameters, the comprehensive temperature deviation formula can be expressed in its final form:

$$\Delta T(w, IS) = \frac{\delta}{\lambda\cdot F_2}\cdot\frac{(1-A)\cdot IS\cdot F_1 - k\left(\frac{IS}{IS_{STC}}\right)^{1.2}\cdot F_3}{0.037\left(\frac{w\cdot\delta}{\nu}\right)^{0.8}\cdot\left(\frac{\nu}{a}\right)^{0.43} + 0.55\left(\frac{g\cdot\beta\cdot\Delta T\cdot\delta^3}{\nu^2}\cdot\frac{\nu}{a}\right)^{0.25}} \quad (7)$$

where: w – wind speed (m·s^{-1}); δ – outer diameter of radiation shield (m); ν – air kinematic viscosity coefficient (m^2·s^{-1}); a – air thermal diffusivity coefficient (m^2·s^{-1}); g – acceleration of gravity (m·s^{-2}); β – volumetric expansion coefficient (K^{-1}); λ – air thermal conductivity coefficient (W·m^{-1}·K^{-1}); 0.037 and 0.55 – empirical coefficients for forced and free convection, respectively; 0.8, 0.43, and 0.25 – exponents derived from heat transfer similarity theory

Derived Eq. (7) has no analytical solution for ΔT. Instead, it can be solved using a fixed-point iteration method with damping technique to ensure stable convergence. The iteration process terminated upon reaching 0.001 °C accuracy between consecutive approximations or after completing the maximum iteration count. Appropriate constraints were implemented in the calculation scheme to handle special cases arising during physical modelling. The solution algorithms were integrated directly into the meteorological station's microcontroller software, enabling real-time temperature correction based on accompanying environmental parameters.

Results and discussion

The mathematical model described in the theoretical framework was applied to analyse the temperature deviation of radiation shields under varying conditions of solar radiation and wind speed. For practical implementation of the model, specific numerical coefficients were determined for the radiation shield used in this study. Table 1 presents these coefficients, which were utilised in the calculations of temperature deviation according to Eq. (7).

Table 1 Numerical coefficients for radiation shield temperature deviation calculations

A	F_1 (m^2)	F_2 (m^2)	F_3 (m^2)	δ (m)	k (W·m^{-2})
0.8	0.015	0.09	0.12	0.14	17.2

Model calculations demonstrate that increasing solar radiation intensity causes elevated temperature readings, while higher wind speeds reduce temperature deviation through enhanced convective heat dissipation. As illustrated in Fig. 4, at a solar radiation intensity of 1000 W·m^{-2} and zero wind speed, the temperature

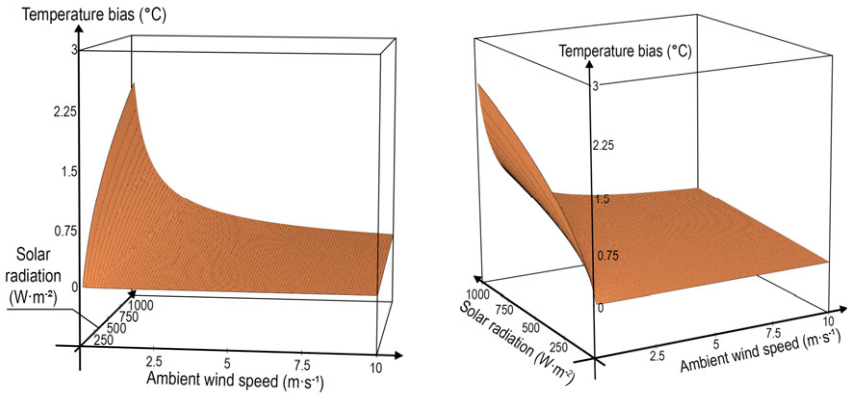


Fig. 4 Air temperature deviation dependence on solar radiation intensity and wind flow speed
Views (a) and (b) show different perspectives for clarity

deviation from the true value reaches 2.3 °C. These simulations were conducted at an ambient temperature of approximately 20 °C, with all thermal coefficients and heat transfer parameters calibrated specifically for this temperature regime. Temperature-dependent variations in air properties (thermal conductivity, kinematic viscosity, and volumetric expansion coefficient) were incorporated in the model to ensure computational accuracy. This numerical simulation result shows the relationship between air temperature deviation, solar radiation intensity, and wind flow speed for the radiation shield under study.

Intercomparison of ASP, NASP, NASPa in relation to RD

The intercomparison utilised statistical metrics and hourly distribution patterns relative to RD. Analysis revealed distinct performance differences among radiation shield configurations. The NASP system demonstrated substantial positive bias exceeding 2 °C during peak radiation periods (10–14 hours), clearly visible in the hourly deviation heatmap (Fig. 5). Conversely, ASP measurements maintained deviations below 1 °C with more uniform error distribution throughout the observation period.

The NASPa approach demonstrated superior performance across all evaluation metrics. The maximum deviations remained within 0.5–0.6 °C and showed no time-dependent bias patterns in the heatmap analysis, indicating effective compensation for solar radiation effects.

Quantitative metrics confirmed these observations, with mean error (ME) values of 0.06 °C for both NASPa and ASP compared to 0.29 °C for NASP. Root mean square error (*RMSE*) values of 0.17 °C, 0.21 °C, and 0.51 °C for NASPa, ASP, and NASP respectively further established this performance hierarchy. The normalised *RMSE* percentages (3.5%, 4.2%, and 10.3%) and Kling–Gupta efficiency (KGE) values (0.993, 0.988, and 0.942) provided additional verification of NASPa's optimal performance (Gupta et al., 2009).

Both ASP and NASPa achieved measurement accuracy within the World Meteorological Organization's permissible

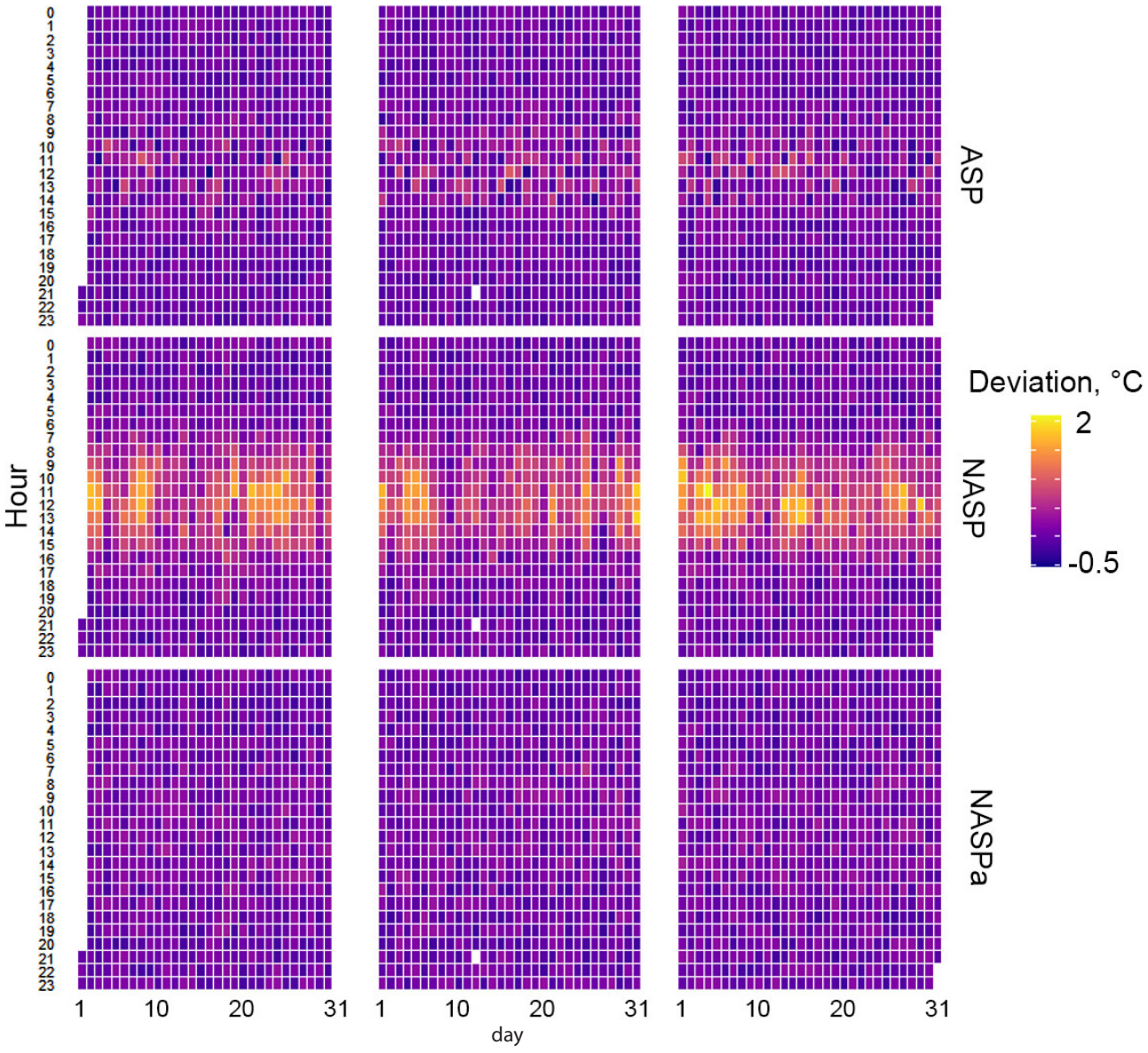


Fig. 5 Heatmap of air temperature deviations for three types of sensors ASP, NASP, NASPa versus RD for June–August 2023

temperature error threshold (0.1 °C), while NASP significantly exceeded this standard. Linear regression analysis revealed near-perfect alignment between NASPa measurements and RD, surpassing the correlation quality observed for both ASP and NASP configurations. The comprehensive assessment establishes that the NASPa algorithm provides superior measurement quality compared to both standard NASP and mechanically aspirated ASP approaches.

Experimental data analysis showed perfect alignment of all devices with RD during nighttime hours, while daytime measurements revealed systematic deviations. During peak solar radiation (10–14 hours), NASP devices exhibited temperature biases up to 3 °C, while ASP systems maintained deviations below 1 °C. This confirms that forced ventilation effectively mitigates radiation-induced measurement errors.

The ASP approach, despite its accuracy advantages, presents two specific drawbacks: an accelerated contamination of internal components requiring more frequent maintenance, and increased system cost with reduced reliability due to additional mechanical elements (Rausand et al., 2021). For permanent meteorological installations, these limitations become critical operational factors.

Prior correction formulas (Hubbard, 2011) and computational fluid dynamics models (Dai et al., 2023) inadequately account for radiation shield design characteristics that determine heat exchange dynamics. These models incorrectly predict temperature deviation patterns when applied to the specific radiation shields tested in this study, particularly underestimating direct solar radiation effects.

This research developed and validated a new temperature correction formula (Eq. 7) incorporating both wind speed and solar radiation intensity parameters with specific geometric shield characteristics. When applied to NASP measurements (creating NASPa data), the correction reduced the maximum deviations up to 0.5–0.6 °C and improved all statistical metrics, including *RMSE* (0.17 °C) and KGE (0.993), which exceeds even ASP performance.

The correction algorithm's limitations occur primarily at the midday maximum insolation (>1000 $W \cdot m^{-2}$), where model simplifications in heat transfer mechanisms introduce residual errors. Nevertheless, the average deviation remains below 0.2 °C, meeting requirements for most agricultural applications. The balance between model complexity and practical accuracy makes the proposed approach particularly suitable for affordable meteorological systems in precision agriculture.

Conclusion

The research demonstrates that adaptive correction methods significantly improve ambient air temperature measurement accuracy using inexpensive meteorological systems. Non-aspirated radiation shields exhibit considerable positive bias in temperature readings during daylight hours, reaching 3 °C above RD due to solar radiation effects. Aspirated shields provide significantly better agreement with reference measurements by maintaining thermal equilibrium between the shield interior and ambient environment.

The alternative correction method, based on calculating temperature bias as a function of solar radiation intensity and wind speed, demonstrated high efficacy with residual deviations not exceeding 0.5–0.6 °C throughout most of the observation period. This approach maintains measurement accuracy comparable to aspirated systems without their mechanical complexity, though it necessitates additional sensors for wind speed and solar radiation intensity measurements.

The methodology presented can be adapted to various radiation shield designs through the experimental determination of model parameters. Widespread implementation of such adjustment algorithms would facilitate the development of affordable, reliable environmental monitoring systems for precision agriculture applications.

It should be emphasised that the presented model has universal theoretical foundations based on dimensionless similarity criteria. The empirical components in the model reflect heat transfer patterns specific to the shield geometry rather than location-dependent climate properties. The calibration parameters (surface albedo, geometric factors, shield diameter, and thermal correction coefficient) characterise only the radiation shield design, making the methodology applicable across different geographical regions when properly calibrated.

Future research should examine these methods over extended observation periods and varied weather conditions. The incorporation of additional parameters such as ambient humidity and internal shield surface temperature could potentially enhance correction accuracy further.

Acknowledgment

The study was supported within the framework of the state assignment of the Ministry of Science and Higher Education of the RF (no. FNZM-2025-0005 "Development of predictive analytics methods and advancement of intelligent technologies in viticulture"). The work of V.E. was supported by the program ‚Prioritet-2030' of SSU (no. 121121700314-3). This research was also supported by Slovak Ministry of Education, Research, Development and Youth within the projects KEGA 012ŽU-4/2025 and VEGA 1/0509/23.

References

ALI, H. – FAROOQUE, A. A. –ABBAS, F. –YAQUB, R. – ABDALLA, A. – SOORA, P. 2024. An IoT based weather monitoring system for smart agriculture. In 2024 IEEE Conference on Technologies for Sustainability (SusTech), Portland, OR, USA, pp. 378–382. DOI: https://doi.org/10.1109/SusTech60925.2024.10553425

Ammoniaci, M. – Kartsiotis, S.-P. – Perria, R. – Storchi, P. 2021. State of the art of monitoring technologies and data processing for precision viticulture. In Agriculture, vol. 11, no. 3, article no. 201. DOI: https://doi.org/10.3390/agriculture11030201

Bergman, T. L. – Lavine, A. S. 2017. Fundamentals of Heat and Mass Transfer. 8th ed. Hoboken, NJ, USA : John Wiley & Sons, Inc., 1045 pp. ISBN 978-1-119-32042-5.

CHEN, S. – GUO, J. – ZHAO, Y. – LI, X. – LIU, F. – CHEN, Y. 2021. Evaluation and grading of climatic conditions on nutritional quality of rice: A case study of Xiaozhan rice in Tianjin. In Meteorological Applications, vol. 28, no. 4, article no. e2021. DOI: https://doi.org/10.1002/met.2021

da Cunha, A. R. 2015. Evaluation of measurement errors of temperature and relative humidity from HOBO data logger under different conditions of exposure to solar radiation. In Environmental Monitoring and Assessment, vol. 187, no. 5, article no. 236. DOI: https://doi.org/10.1007/s10661-015-4458-x

Dai, W. – Tan, M. – Zhu, H. 2023. Design of a radiation shield applied to surface air temperature monitoring. In Journal of Instrumentation, vol. 18, article no. P02015. DOI: https://doi.org/10.1088/1748-0221/18/02/P02015

EL HACHIMI, C. – BELAQZIZ, S. – KHABBA, S. – SEBBAR, B. – DHIBA, D. – CHEHBOUNI, A. 2023. Smart weather data management based on artificial intelligence and big data analytics for precision agriculture. In Agriculture, vol. 13, no. 1, article no. 95. DOI: https://doi.org/10.3390/agriculture13010095

Erell, E. – Leal, V. – Maldonado, E. 2005. Measurement of air temperature in the presence of a large radiant flux: An assessment of passively ventilated thermometer screens. In Boundary-Layer Meteorology, vol. 114, pp. 205–231. DOI: https://doi.org/10.1007/s10546-004-8946-8

Ferrández-Pastor, F. J. – García-Chamizo, J. M. – Nieto-Hidalgo, M. – Mora-Martínez, J. 2018. Precision agriculture design method using a distributed computing architecture on Internet of Things context. In Sensors, vol. 18, no. 6, article no. 1731. DOI: https://doi.org/10.3390/s18061731

FRISVOLD, G. B. – MURUGESAN, A. 2013. Use of weather information for agricultural decision making. In Weather, Climate and Society, vol. 5, no. 1, pp. 55–69. DOI: https://doi.org/10.1175/WCAS-D-12-00022.1

Georges, C. – Kaser, G. 2002. Ventilated and unventilated air temperature measurements for glacier-climate studies on a tropical high mountain site. In Journal of Geophysical Research: Atmospheres, vol. 107, no. D24, pp. ACL 15-1–ACL 15-10. DOI: https://doi.org/10.1029/2002JD002503

Gupta, H. V. – Kling, H. – Yilmaz, K. K. – Martinez, G. F. 2009. Decomposition of the mean squared error and NSE performance criteria: Implications for improving hydrological modelling. In Journal of Hydrology, vol. 377, no. 1–2, pp. 80–91. DOI: https://doi.org/10.1016/j.jhydrol.2009.08.003

HOLLEMAN, C. – REMBOLD, F. – CRESPO, O. – CONTI, V. 2020. The impact of climate variability and extremes on agriculture and food security – An analysis of the evidence and case studies. Background paper for The State of Food Security and Nutrition in the World 2018. In FAO Agricultural Development Economics Technical Study No. 4. Rome, FAO, 108 pp. DOI: https://doi.org/10.4060/cb2415en

Hubbard, K. G. – Lin, X. 2002. Realtime data filtering models for air temperature measurements. In Geophysical Research Letters, vol. 29, no. 10, pp. 67-1–67-4. DOI: https://doi.org/10.1029/2001GL013191

Hubbard, K. G. – Lin, X. – Walter-Shea, E. A. 2001. The effectiveness of the ASOS, MMTS, Gill, and CRS air temperature radiation shields. In Journal of Atmospheric and Oceanic Technology, vol. 18, no. 6, pp. 851–864. DOI: https://doi.org/10.1175/1520-0426(2001)018<0851:TEOTAM>2.0.CO;2

Hubbart, J. A. 2011. An inexpensive alternative solar radiation shield for ambient air temperature micro-sensors. In Journal of Natural & Environmental Sciences, vol. 2, no. 2, pp. 9–14.

Ioannou, K. – Karampatzakis, D. – Amanatidis, P. – Aggelopoulos, V. – Karmiris, I. 2021. Low-cost automatic weather stations in the Internet of Things. In Information, vol. 12, no. 4, article no. 146. DOI: https://doi.org/10.3390/info12040146

Jenkins, G. 2014. A comparison between two types of widely used weather stations. In Weather, vol. 69, no. 4, pp. 105–110. DOI: https://doi.org/10.1002/wea.2158

Kuznetsov, P. N. – Kotelnikov, D. Y. – Shchekin, V. Y. – Koltsov, A. D. – Kabankova, E. N. 2022. Intelligent complex of monitoring and diagnostics of grape plantations. In IOP Conference Series: Earth and Environmental Science, vol. 981, no. 3, article no. 032020. DOI: https://doi.org/10.1088/1755-1315/981/3/032020

MARMAI, N. – FRANCO VILLORIA, M. – GUERZONI, M. 2022. How the Black Swan damages the harvest: Extreme weather events and the fragility of agriculture in development countries. In PLOS ONE, vol. 17, no. 2, article no. e0261839. DOI: https://doi.org/10.1371/journal.pone.0261839

Matese, A. – Di Gennaro, S. F. – Zaldei, A. – Genesio, L. – Vaccari, F. P. 2009. A wireless sensor network for precision viticulture: The NAV system. In Computers and Electronics in Agriculture, vol. 69, no. 1, pp. 51–58. DOI: https://doi.org/10.1016/j.compag.2009.06.016

Onesti, G. – González-Domínguez, E. – Rossi, V. 2016. Accurate prediction of black rot epidemics in vineyards using a weather-driven disease model. In Pest Management Science, vol. 72, no. 12, pp. 2321–2329. DOI: https://doi.org/10.1002/ps.4277

Rausand, M. – Barros, A. – Hoyland, A. 2021. System Reliability Theory: Models, Statistical Methods, and Applications. 3rd ed. Hoboken, NJ, USA : John Wiley & Sons, Inc., 845 pp. eISBN 9781119373940. DOI: https://doi.org/10.1002/9781119373940

Richardson, S. J. – Brock, F. V. – Semmer, S. R. – Jirak, C. 1999. Minimizing errors associated with multiplate radiation shields. In Journal of Atmospheric and Oceanic Technology, vol. 16, no. 11, pp. 1862–1872. DOI: https://doi.org/10.1175/1520-0426(1999)016<1862:MEAWMR>2.0.CO;2

Sun, X. – Yan, S. – Wang, B. – Xia, L. – Liu, Q. – Zhang, H. 2015. Air temperature error correction based on solar radiation in an economical meteorological wireless sensor network. In Sensors, vol. 15, no. 8, pp. 18114–18139. DOI: https://doi.org/10.3390/s150818114

Tarara, J. M. – Hoheisel, G.-A. 2007. Low-cost shielding to minimize radiation errors of temperature sensors in the field. In HortScience, vol. 42, no. 6, pp. 1372–1379. DOI: https://doi.org/10.21273/HORTSCI.42.6.1372

Yang, J. – Deng, X. – Liu, Q. – Ding, R. 2021. Design and experimental study of an effective, low-cost, naturally ventilated radiation shield for monitoring surface air temperature. In Meteorology and Atmospheric Physics, vol. 133, no. 2, pp. 349–357. DOI: https://doi.org/10.1007/s00703-020-00754-1

Yang, J. – Liu, Q. – Dai, W. 2018. A method for solar radiation error correction of temperature measured in a reinforced plastic screen for climatic data collection. In International Journal of Climatology, vol. 38, no. 3, pp. 1328–1336. DOI: https://doi.org/10.1002/joc.5247

Yang, J. – Liu, Q. – Dai, W. – Ding, R. 2016. A temperature error correction method for a naturally ventilated radiation shield. In Journal of Atmospheric and Solar-Terrestrial Physics, vol. 149, pp. 40–45. DOI: https://doi.org/10.1016/j.jastp.2016.09.010

Yang, S.-H. – Lee, C.-G. – Kim, J.-Y. – Lee, W.-K. – Ashtinai-Araghi, A. – Rhee, J.-Y. 2012. Effects of fan-aspirated radiation shield for temperature measurement in greenhouse environment. In Journal of Biosystems Engineering, vol. 37, no. 4, pp. 245–251. DOI: https://doi.org/10.5307/JBE.2012.37.4.245

WORLD METEOROLOGICAL ORGANIZATION (WMO). 2023. Guide to Instruments and Methods of Observation, Volume I – Measurement of Meteorological Variables. Preliminary 2023 edition of WMO-No. 8. Geneva, Switzerland. Available at: https://community.wmo.int/en/activity-areas/imop/wmo-no.8/preliminary-2023-edition-wmo-no-8

ZHANG, X. – CHEN, K. – LI, K. 2023. Detection of meteorological influence on bread wheat quality in Hebei province, China based on the gradient boosting decision tree. In Frontiers in Plant Science, vol. 14, article no. 1083665. DOI: https://doi.org/10.3389/fpls.2023.1083665